Optimization of Sluice Box for Small-Scale Mining Using Computational Fluid Dynamics (CFD)*

[1]E. Yin, [1]E. Taylor, [2]E. Quaicoe and [1]E. K. Asiedu
[1]University of Mines and Technology, P.O. Box 237, Tarkwa, Ghana
[2]Department of Mechatronics and Robotics Engineering, School of Innovative Design Engineering, Egypt-Japan University of Science and Technology, P.O. Box 179, New Borg El-Arab City, Alexandria, Egypt

Yin, E., Taylor, E., Quaicoe, E. and Asiedu, E. K. (2024), "Optimization of Sluice Box for Small-Scale Mining Using Computational Fluid Dynamics (CFD)", *Ghana Mining Journal*, Vol. 24, No. 1, pp. 178-187.

Abstract

The issue of gold losses to tailings leading to low recovery in the artisanal and small-scale mining industries, which mostly rely on traditional sluicing techniques to concentrate gold particles from gangue minerals, remains critical. This research contributes to improving gold recovery by optimizing the sluice box design to improve its efficiency. Based on the multi-stage sluice box system proposed in prior work done, Computational Fluid Dynamics (CFD) simulations was performed by varying the slope angles of the sluice box to determine the optimal angle that will produce the highest recovery of gold concentrates from the gangue minerals. The results obtained demonstrated that the optimal slope angle of the sluice box that retained most gold particles was 10°. At this slope angle, the gold retention rate, flow velocity, and the number of gold particles trapped on the sluice box were 98.81 %, 0.311 m/s, and 7905 particles, respectively. This study, therefore, provides the foundation for numerical technique (CFD) to be used for analyzing fluid flow on a sluice box to complement experimental and empirical techniques.

Keywords: Multiphase flow, CFD, Optimization, Small-scale mining, Sluice box, SolidWorks, Gold recovery.

1 Introduction

In many parts of the world, especially in developing nations like Ghana that are endowed with gold, artisanal and small-scale gold mining is a frequent and substantial economic activity that serves as a source of employment and livelihood for many. However, the current state of gold recovery in these mines, characterized by poor recovery due to less efficient mining methods and tools, is a pressing issue. The simple, less efficient, traditional sluice box techniques are predominantly used by artisanal and small-scale gold miners to recover or concentrate gold particles from the gangue minerals, leading to gold losses and low recovery. The urgency of this issue underscores the importance of our research in optimizing the efficiency of the sluice box system, which could significantly improve gold recovery rates.

Sluice boxes are hydraulic structures that regulate and control the flow of water (Simmons and Brown, 2014). They are frequently employed by artisanal and small-scale miners for recovery because they are easier to use, cost-effective, and have fewer negative environmental impacts than mercury amalgamation techniques (Hilson, 2002). In the sluicing technique, gold is separated from other materials by placing the ore onto the sluice box and allowing water to flow over it. As the water flows over the box, it creates a fluidized bed, which separates the gold from the other gangue materials by taking advantage of the differences in their densities (Banisi and Hadizadeh, 2008).

The efficiency of a sluice box in retaining or capturing gold particles during the recovery process lies in its design parameters (length and width), the angle of slope, the water flow rate, and the characteristics of the ore being processed (Mular *et al.*, 2002). The sluice box must allow water to flow on it at a controlled rate. Unfortunately, the design of these traditional sluice boxes employed in most artisanal and small-scale mining sites is largely based on trial and error. For instance, in Tarkwa, Ghana, where the ore deposit is mostly alluvial, these traditional sluicing techniques are commonly employed to concentrate the gold. Fig. 1 shows a traditional sluicing method at a small-scale mine site in Tarkwa, Ghana. This yields many losses of the gold to the tailings, resulting in low or poor recovery.

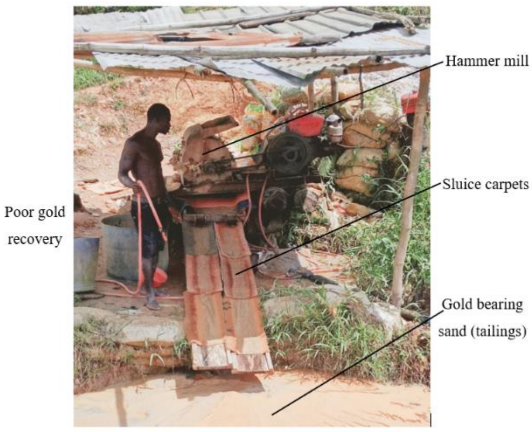

Fig. 1 Setup of a Hammer Mill and a Traditional Sluice System (Yin *et. al.* 2020a)

*Manuscript received February22, 2024
Revised version accepted June 15, 2024
https://doi.org/10.4314/gm.v22i1.3

The need to increase the recovery of gold has resulted in several different techniques for extracting or recovering the gold in both small-scale and large-scale mines. The use of long leaching time and a Carbon-in-Leach (CIL)/Carbon-in-Pulp (CIP) recovery system may eliminate the need for gravity concentration, but the gravity concentration method has recently gained attention and has been seen as an inexpensive way of improving the recovery on existing plants (Lovedayt, 1982).

Several research have used actual experiments to look at the flow characteristics of sluice boxes. A review of the literature is necessary as it elaborates on progress made on the subject matter, the various methodologies employed, and the research gap (Yin *et. al.*2020b)

Oyuntsetseg and Altantuya (2007), in their experimental work, studied the flow and particle trajectories of slurry on a sluice box. They discovered that the riffle height and spacing have an impact on the sluice box's separation effectiveness and level of turbulence. They discovered that the optimal riffle spacing, and angle of riffle were 8.5 mm and 107º respectively.

Stewart and Ramsay (1993) conducted experimental studies that described how the design of a sluice box could be modified to improve its effectiveness so that both the grade and recovery of fine heavy minerals (fine gold) can be improved. In presenting their experimental results, they concluded that once the flow rate in the sluice box is great enough to maintain most of the solids in suspension, then the solid is retained in the box in quiescent (dead) zones. The size of these zones is dependent on flow patterns within the box, which in turn are mainly dependent on box geometry. Increasing the sluice-box slope increases the flow rate but causes a reduction in the dead space, which can cause a decrease in recovery. They also concluded that sluice boxes could be improved to increase both grade and recovery by the riffles design in a manner that establishes the dead zone and optimizes movement in the dead zone.

Additional research also concentrated on how particle size distribution and bed thickness affect sluice box flow parameters and gold recovery effectiveness. Alabi and Gbadamosi (2021) experimented with a small-scale sluice box with various particle sizes and bed thicknesses. Due to the higher sedimentation velocity and longer residence times of smaller particles, they discovered that the gold recovery rate rose with decreasing particle size and growing bed thickness. They did note, however, that with thicker beds and finer particles, water consumption and environmental impact rose.

Agyei and Gordon (2017) investigated the impact of riffle height and spacing on gold recovery in a sluice box. They found that both factors significantly impact the recovery of the gold particles. At a riffle height and spacing of 1.0 cm and 15 cm, respectively, an appreciable percentage of gold was recovered for the indicated velocities of flow and the spacing.

Other related works have investigated the use of advanced materials and coatings to enhance the performance and durability of sluice boxes. Hamilton (1988) examined the flow and erosion patterns in a sluice box with various kinds of matting and coatings in his experiment. In comparison to traditional rubber matting and steel coatings, they discovered that the use of polyurethane matting and ceramic coatings boosted gold recovery rates and decreased sluice box wear and tear.

Some researchers have also investigated the use of other sluice box designs and arrangements, including shaking tables, centrifugal concentrators, and pulsating jigs. These machines use various fluid mechanics and sedimentation processes to separate gold particles from other materials. Kelly *et al*. (1995) optimized the design and operational parameters of a pulsating jig for gold recovery using experiments. In comparison to typical sluice boxes, they discovered that raising the pulsation frequency and amplitude increased the separation efficiency and decreased water use.

Some studies have investigated the potential of combining different technologies and approaches to improve the overall efficiency and sustainability of small-scale gold mining. Veiga et al. (2006) tested the utilization of mercury-free gold extraction techniques, such as gravity concentration, cyanidation, and flotation, through field studies in several nations. They discovered that despite lowering the dangers to the environment and human health associated with mercury use, these techniques could produce gold recovery rates that were on par with or higher than mercury amalgamation.

Empirical equations have been developed to predict the performance of sluice boxes based on the geometry of the box and the properties of the ore. One such equation is the Deister formula, which relates the length and width of the box to the maximum particle size that can be effectively trapped by the riffles (Mular *et al*., 2002). Other empirical equations include the Froude number equation,

$$Fr = \frac{v}{\sqrt{gl}} \tag{1}$$

Where:

Fr = Froude number
v = average velocity of liquid in channel
g = acceleration due to gravity

The top width of the water surface and the velocity coefficient equation relates the water flow rate to the effectiveness of the box (Banisi and Hadizadeh, 2008).

Despite the availability of these various methods, CFD simulations have been limitedly applied to the analysis of sluice boxes. This is likely due to the box's complex geometry and the highly nonlinear nature of the flow and particle transport processes involved. However, recent advances in CFD technology, including improvements in meshing algorithms and turbulence models, have made it feasible to perform detailed simulations of these systems.

In a variety of engineering applications, computational fluid dynamics (CFD) is a powerful numerical technique used to evaluate fluid flow behaviour and evaluate fluid performance. It entails using numerical methods on a computational domain to solve the Navier-Stokes equations and other governing equations of fluid flow. CFD can precisely mimic fluid behaviour and produce detailed information on factors like pressure, velocity, temperature, and turbulence by discretizing the domain into a large number of small control volumes or computational cells.

SolidWorks flow simulation is one of the most widely used CFD software packages in the engineering industry. It has a wide range of capabilities, including the ability to simulate turbulent, multiphase, and compressible fluid flows, as well as heat transfer. It also offers various turbulence models and numerical methods for simulating different flow regimes. These features make SolidWorks simulation an ideal choice for simulating the fluid flow through the sluice box in this project. Computational analysis has gained much interest in mechanical engineering as it provides solutions to a variety of problems in the areas of design, manufacturing, optimization, fluid flow, energy, etc. Researchers (Yin *et. al.* 2024) used computational analysis to validate analytical results in their study.

To increase the recovery of gold, it is necessary to optimize the flow characteristics of the sluice box. This necessitates a thorough comprehension of the flow patterns over a plate, velocity, slope angle, and turbulence of the water and sediment mixture. Most current efforts to design and optimize sluice boxes rely on empirical methods, which can lead to less-than-ideal designs that fail to take into consideration the intricate flow dynamics within the sluice box.

The slope of the sluice box is a design parameter that affects the flow behaviour and separation efficiency of the system. Although much work has been done experimentally, the optimal angle that can ensure that the sluice box operates at maximum efficiency has not yet been investigated computationally. This work seeks to minimize gold losses and improve gold recovery by using CFD to optimize the gold recovery process using sluice boxes in small-scale mining. The use of CFD enables the prediction and visualization of fluid and particle behaviour in various sluice box regions under a variety of situations, including varying slope angles, fluid flow rates, and riffle designs. The geometry of the sluice box is crucial to its performance, as it determines the flow behaviour of the fluid and the separation efficiency of the system. The main objective of this study is to employ computational fluid dynamics (CFD) to obtain the optimal slope angle and velocity for which maximum gold recovery can be extracted from the sluice box.

2 Methodology

Figs. 2 and 3 show the isometric and the exploded views of the multi-stage sluice box design proposed in our prior work (Yin *et. al.* 2020a), whereas Table 1 shows the part list.

Fig. 2 Isometric View of Optimized Design (Yin *et. al.* 2020a)

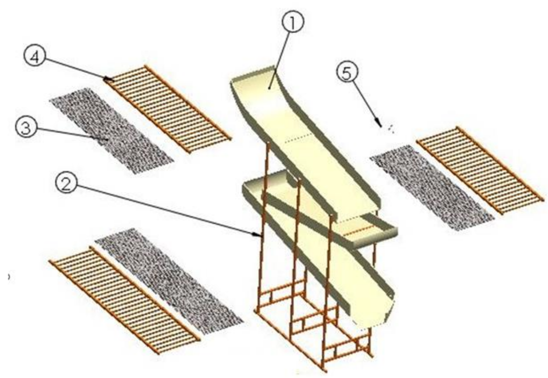

Fig. 3 Exploded View of Optimized Design (Yin *et. al.* 2020a)

Table 1 Part list

No.	Item Name	Material Description	Qty
1	Sluice channel	Aluminium	3-sets
2	Sluice support frames	Grey cast iron	6
3	Carpets/Mats	Miner's moss	3
4	Riffles	Aluminium	3-sets
5	Machine screws	Steel	12

2.1 Mass of Pulp to be Leached.

The mass of pulp to be leached is given by equation (2),

$$M_{pulp} = V_{pulp} \times \rho_{pulp} \tag{2}$$

Where,

ρ_{pulp} = Pulp density.

Assuming the slurry is thickened to a pulp of 46% solids, $\rho_{pulp} = 1400 \text{ kg/m}^3$ (Kotze *et al*., 2005).

By substitution,

$$M_{pulp} = 900 \text{ kg}$$

Neglecting the mass of gold concentrates trapped by the carpets and riffles after sluicing, the mass of solid ore (M_{solids}) to be processed at a time on the sluice box was estimated as:

$$M_{\text{solids}} = \text{Percentage solids} \times M_{pulp} \tag{3}$$

By substitution,

$$M_{solids} = \frac{46}{100} \times 900$$

$$M_{solids} = 415 \text{ kg}$$

The sluice channel comprises a pair of side walls and a flat bottom, which are operatively connected to the side walls. Riffles (0.03 m high, 0.2 m apart) are operatively connected to the bottom of the channels. According to Veiga et al. (2006), three 2 m zigzag sluices (each inclined at 10°) are usually better than one single 6 m sluice as increased kinetic energy in long sluices decreases recovery. Per the design considerations, material and space requirements, the sluice channels have the following outer dimensions:

Length of channel (l_c) = 2 m

Width of channel (w_c) = 0.5 m

Height of channel side walls (h_c) = 0.25 m

Thickness of channel (t_c) = 0.003 m

Fig. 4 shows the exploded view of the sluice box design.

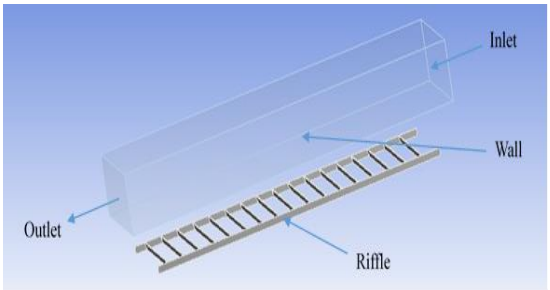

Fig. 4 Exploded View of the Sluice Box

In the Eulerian-Eulerian approach, two phases are considered to be interpenetrating. SolidWorks Flow Simulation uses the Euler-Euler multiphase flow model to simulate solid-liquid multiphase flows. With this approach, the continuity and momentum equations are solved for each phase, and therefore, the determination of separate flow field solutions is allowed.

In fluid regions, SolidWorks flow simulation solves the Navier-Stokes equations, which are formulations of mass, momentum, and energy conservation laws. These equations are used to mathematically describe the physics of fluid flow. The continuity equation and the momentum equation, also known as the Navier-Stokes equation, are needed to describe the state of any type of flow and are generally solved for all flows in CFD modelling (Stenmark, 2013).

The Continuity Equation (Conservation of Mass) equation is as stated in (4),

$$\frac{\partial \rho}{\partial t} + \frac{\partial (\rho u_i)}{\partial x_i} = 0 \tag{4}$$

Where,

ρ is the phase density.

t is the time.

u is the phase velocity.

The Conservation of Momentum equation is as stated in (5).

$$\frac{\partial \rho u_i}{\partial t} + \frac{\partial}{\partial x_j}(\rho u_i u_j) + \frac{\partial P}{\partial x_i} = \frac{\partial}{\partial x_i}(\tau_{ij} + \tau_{ij}^R) + S_i \tag{5}$$

SolidWorks flow simulation considers both laminar and turbulent flows. Laminar flows occur at low values of the Reynolds number, which is defined as the product of representative scales of velocity and length divided by the kinematic viscosity. When the Reynolds number exceeds a certain critical value, the flow transitions smoothly to turbulent. To predict turbulent flows, the Favre-averaged Navier-Stokes equations is used, where time-averaged effects of the flow turbulence on the flow parameters are considered, whereas the large-scale, time-dependent phenomena are considered directly.

Through this procedure, extra terms known as the Reynolds stresses appear in the equations for which additional information must be provided. To close this system of equations, SolidWorks flow simulation employs transport equations for the turbulent kinetic energy and its dissipation rate using the k-ε model (Sobachkin and Dumnov, 2014).

The modified k-ε turbulence model with damping functions proposed by Lam and Bremhorst, 1981 describes laminar, turbulent, and transitional flows of homogeneous fluids consisting of the following turbulence conservation laws:

$$\frac{\partial \rho k}{\partial t}+\frac{\partial \rho k u_i}{\partial x_i}=\frac{\partial}{\partial x_i}\left(\mu+\frac{\mu_i}{\sigma_k}\right)\frac{\partial k}{\partial x_i}+\tau_{ij}^{R}\frac{\partial u_i}{\partial x_j}-\rho\varepsilon+\mu_t P_B \quad (6)$$

$$\frac{\partial \rho\varepsilon}{\partial t}+\frac{\partial \rho\varepsilon u_i}{\partial x_i}=\frac{\partial}{\partial x_i}\left(\mu+\frac{\mu_i}{\sigma_k}\right)\frac{\partial k}{\partial x_i}+C_{\varepsilon l}\frac{\varepsilon}{k}\left(f_1\tau_{ij}^{R}\frac{\partial u_i}{\partial x_j}+C_{\varepsilon}\mu_t P_B\right)-f_2 C_{\varepsilon 2}\frac{\rho\varepsilon^2}{k} \quad (7)$$

$$\tau_{ij}=\mu s_{ij},\tau_{ij}^{R}=\mu_t s_{ij}-\frac{2}{3}\rho k\delta_{ij},s_{ij}=\frac{\partial u_i}{\partial x_j}+\frac{\partial u_j}{\partial x_i}-\frac{2}{3}\delta_{ij}\frac{\partial u_k}{\partial x_k} \quad (8)$$

$$P_B=-\frac{g_i}{\delta_B}\frac{1}{\rho}\frac{\partial \rho}{\partial x_i} \quad (9)$$

Where:

$$C_\mu=0.09 \quad C_{\varepsilon l}=0.09 \quad C_{\varepsilon L}=1.92$$

$$\delta_k=1,\ \delta_E=1.3,\ \delta_B=0.9$$

$$C_D=1,\ \text{if } P_B>0,\ \text{and } C_B=0 \text{ if } P_B<0$$

The turbulent viscosity is determined from:

$$\mu_t=f_\mu\cdot\frac{C_\mu\rho k^2}{\varepsilon} \quad (10)$$

Lam and Bremhorst's (1981) damping function f is determined from:

$$f_\mu=\left(1-e^{-0.025R_y}\right)^2\cdot\left(1+\frac{20.5}{R_t}\right) \quad (11)$$

Where:

$$R_y=\frac{\rho\sqrt{k}y}{\mu}$$

$$R_t=\frac{\rho k^2}{\mu\varepsilon}$$

y is the distance from the point to the wall.

For the final results to be obtained, there were a number of procedures that had to be followed for the simulation, which included:

i. Computer-Aided Design (CAD), specifically SolidWorks, was used to model the sluice box to accurate dimensions, as shown in Fig. 5.

ii.

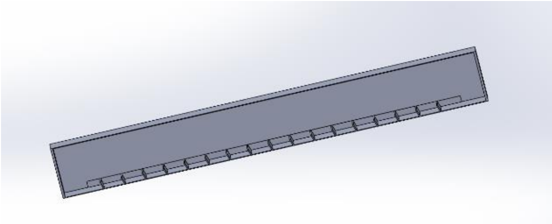

Fig. 5 CAD Drawing

iii. The drawn model was then imported into the SolidWorks Simulation flow.

iv. Meshing was done for the purpose of discretization of the geometry into small elements to allow for numerical computations using an element size of 0.002 m. Fig. 6 and Table 2 show the meshed sluice box and its statistics, respectively.

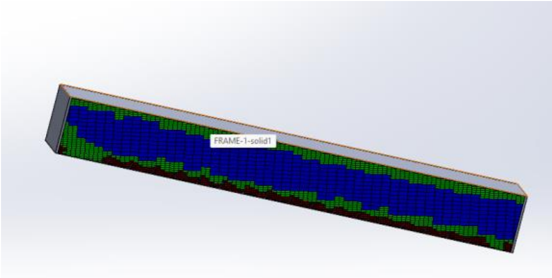

Fig. 6 Meshed Model

Table 2 Mesh Statistics

Entity	Nodes	Elements	Type
Body	44388	234317	solid
Riffle	9408	23882	solid

v. The Solving Process was initiated where the multiphase, discrete model, and boundary conditions were selected and defined. The boundary conditions used include:

Inlet Boundary Condition:

The inlet boundary condition represents the flow rate and velocity of the slurry entering the sluice box. In the simulation, the inlet boundary condition was modeled as a 'velocity inlet' with a specified flow rate. The flow rate was chosen based on the experimental data from Table 3 obtained from the actual sluice box operation. The velocity profile at the inlet was assumed to be uniform, which is a reasonable assumption since the slurry is typically well-mixed before entering the sluice box.

Table 3 Experimental Data for Different Inclination Angles and Feed Rate (Alabi and Gbadamosi, 2021)

Inclination Angle (deg.)	Feed Weight (g)	Concentrate weight (g)	Tailing weight (g)	Feed Assay (ppm)	Concentrate assay (ppm)	% Recovery
10	100	21.70	78.30	10.15	43.2	92.36
20	100	16.40	83.60	10.15	38.97	62.97
30	100	5.90	94.10	10.15	53.01	30.81
40	100	9.70	90.30	10.15	71.37	68.21
50	100	11.88	88.12	10.15	53.36	62.45
60	100	19.44	80.56	10.15	50.04	95.84

Feed Rate (kg/hr)	Weight of Crude (g)	Weight of Concentrate (g)	Weight of Tailings (g)	Assay of Concentrate (ppm)	Assay of Tailings (ppm)
50	100	56.32	43.63	12.83	9.36
60	100	52.99	47.01	26.83	10.83
70	100	32.57	67.43	93.14	6.379
80	100	16.66	83.34	25.32	2.52
90	100	47.39	52.61	27.42	8.01
100	100	41.68	58.32	47.145	7.02

From Table 3, the experiment was conducted at an inlet flow velocity of 0.22 m/s thus the inlet flow velocity of the slurry was set at that value.

Outlet Boundary Condition:

The outflow boundary condition represents the pressure and flow rate of the slurry leaving the sluice box. The outlet boundary condition was simulated as a 'pressure outlet' with a zero-gauge pressure. For this condition to hold true, the exit pressure must match the atmospheric pressure. Based on the flow rate at the intake and the mass conservation principle, the flow rate at the outlet was estimated.

Wall Boundary Condition:

The walls of the sluice box were modeled as 'no-slip' walls, meaning that the velocity at the wall was zero. This boundary condition assumes that the slurry particles are in contact with the wall and do not slip past it. The wall boundary condition was important in ensuring that the simulation accurately captured the flow details near the walls of the sluice box.

vi. The post-processing step, which involves analysing and displaying the simulation data to obtain insights into the flow behaviour and identify areas for sluice box design improvement, is very important for optimizing the sluice box.

4 Result and Discussion

Velocity contours were generated by plotting the velocity over the entire sluice box domain. The contours were useful in visualizing the flow patterns in the sluice box, identifying areas of high and low velocity, and determining areas of potential gold deposition. The velocity contours were also used to calculate the turbulence intensity and Reynolds stresses, which provided insights into the turbulence characteristics of the flow.

Particle tracking was used in the post-processing step to visualize the flow behaviour and identify areas of potential gold deposition. Particle tracking involves tracking the movement of individual particles in the flow. This technique allowed us to identify areas where the slurry was stagnating, and gold particles were likely to settle.

Turbulence intensity and Reynolds stresses were calculated as part of the post-processing step to evaluate the turbulence characteristics of the flow. Turbulence intensity represents the fluctuations in the velocity of the flow, while Reynolds stresses represent the momentum transfer between different parts of the flow. These parameters were used to identify areas of high turbulence and modify the sluice box design to reduce turbulence and improve gold recovery.

The simulation was done to determine which slope angle would trap more gold particles as the slurry flows through the sluice box. The sluice box was modelled with different slope angles ranging from 5° to 20° for the simulations. For each angle, 8402 iterations were carried out. The size of the sluice box, the water flow rate, and the characteristics of the particles were all taken into account throughout each iteration. The number of iterations specified is 8240 (i.e., 600s physical time). The flow was modelled as a transient flow since it is time-dependent; therefore, there is a need to specify time steps.

4.1 Velocity Distribution

One important parameter in the design of a sluice is the distribution of the flow velocity. The results from the simulation provided important insights into how fluid flow behaved in the sluice box at various inclination angles. Fig. 7 to Fig. 10 shows the velocity distribution across the sluice box for various angles of inclination and the maximum velocities reached. The velocities obtained from the SolidWorks simulation for the angles 5 º, 7º, 10º, 15º and 20º, were 0.298, 0.301, 0.311, 0.320 and 0.325 m/s respectively.

The simulation results obtained, summarised, and presented in Table 4, show that the fluid's velocity increases as the angle of inclination increases, i.e., 0.298 m/s to 0.325 m/s. This is because a steeper gradient causes a stronger gravitational force to propel the flow of water down the sluice box. As the angle increases, the gold particles tend to follow the flow direction more closely because of the corresponding increase in flow velocity, which was in agreement with available theories hence, validating the results obtained for the velocity graphs.

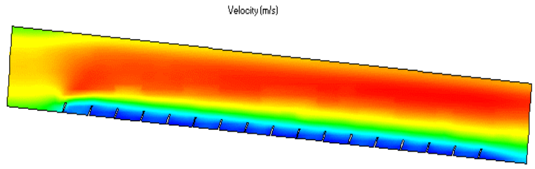

Fig. 7 Velocity Contour Profile for 5º Inclination

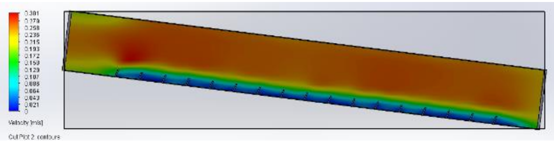

Fig. 8 Velocity Contour Profile for 7º Inclination

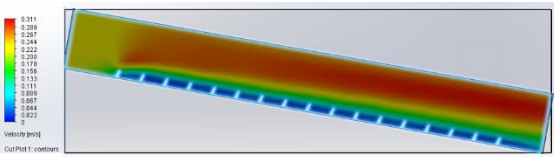

Fig. 8 Velocity Contour Profile for 10º Inclination

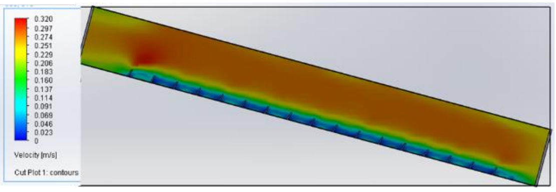

Fig. 9 Velocity Contour Profile for 15º Inclination

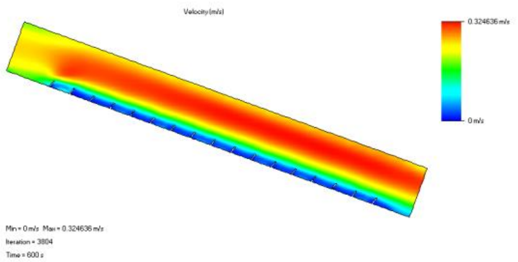

Fig. 10 Velocity Contour Profile for 20º Inclination

4.2 Gold Particle Trajectory

In order to understand how the gold particles, move within the sluice box, individual particles of varying sizes (45 µ*m* to 500 µ*m*) were tracked. 1000 particles were injected for each gold size from the inlet of the sluice box during the simulation. In total, 8000 particles were injected into the inlet. The Fig. 11 to Fig. 15 show the particle trajectories at different angles. for the angles 5 º, 7º, 10º, 15º and 20º, were 7890, 7891, 7905, 7902 and 7888 particles respectively. It was observed that the number of particles trapped was on the ascendancy up until 10º angle with 7905 number of particles trapped and reduced as the slope angle was increased beyond 10º.

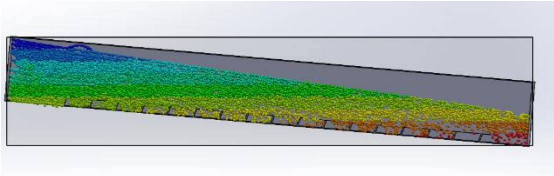

Fig. 11 Particle Trajectory Profile for 5º Inclination

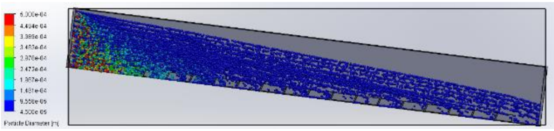

Fig. 12 Particle Trajectory Profile for 7º Inclination

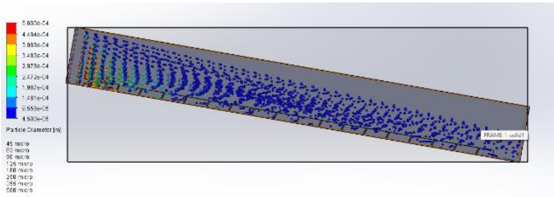

Fig. 13 Particle Trajectory Profile for 10º Inclination

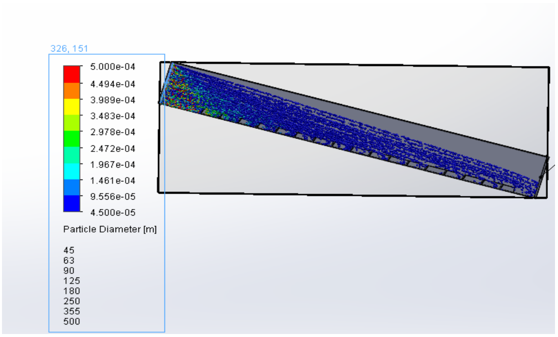

Fig. 14 Particle Trajectory Profile for 15º Inclination

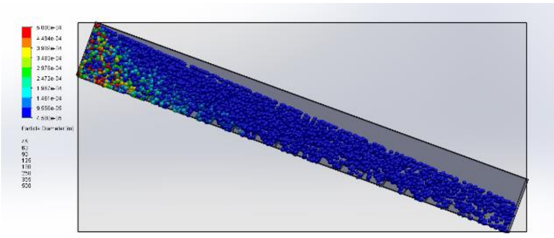

Fig. 15 Particle Trajectory Profile for 20º Inclination

Table 4 shows the results indicating the maximum velocity and the number of particles trapped after the simulations for the different angles were completed.

Table Error! No text of specified style in document. **Particle Recovery and Velocity for Different Slope Angles**

Angle of inclination º	Maximum velocity m/s	Particles Trapped	% Recovery

5	0.298	7890	98.63
7	0.301	7891	98.64
10	0.311	7905	98.81
15	0.320	7902	98.78
20	0.325	7888	98.60

Fig. 16 shows a plotted graph of velocity versus the slope angle. Higher velocities tend to prevent the particles from settling quickly but rather following the flow direction downstream to the tailings, therefore, reducing its recovery rate as shown in Fig. 17. However, the number of particles trapped increased from 7890 to 7905 particles for slope angles between 5º and 10º but decreased as the slope angle was increased beyond 10º as shown in Fig. 16, and this agreed with experimental results obtained by Veiga *et. al.* 2004 and Alabi and Gbadamosi, (2021) who experimentally deduced that the optimal sluice slope angle for maximum gold recovery was 10º hence validating simulation results. The optimal slope angle for maximum gold particles recovery was 10º with of 98.81 % of gold particles recovery.

Therefore, the higher the slope angle, the higher the maximum velocity, but the recovery rate increased to 98.81 % for slope angles below 10º but reduced as the slope angle increased beyond 10º, resulting in a lower recovery rate of the sluice box. Most of the fine gold particles (45 μm) were carried away to the tailings because of their lightweight, while the heavy particles like the 500 μm particles were trapped in all the cases. This therefore implies that small scale miners must ensure that the slope angle for the sluice box should be 10 º if they are to extract maximum amount of gold from their ore.

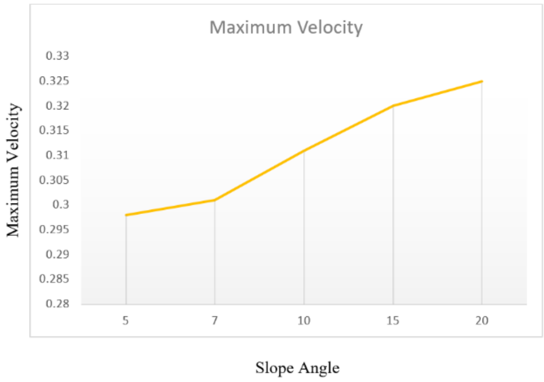

Fig. 16 A Graph of Velocity Versus Slope Angle

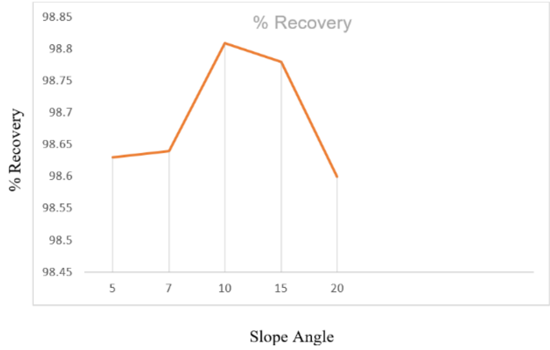

Fig. 17 A Graph of Slope Angle Versus Recovery

5 Conclusion

Comprehensive computational analysis using CFD has been carried out on the sluice box for small-scale mines to deduce the optimal sluice slope angle for maximum gold recovery. Based on the results obtained, the optimal sluice slope angle for maximum gold recovery was 10º with a flow velocity of 0.311 m/s. For a 10º slope angle, the number of particles trapped was 7905 out of 8000 particles, which amounts to 98.81 % gold recovery.

This result agreed with other experimental results from other research works carried out in that their maximum slope angle obtained was 10º. It was therefore recommended that small-scale miners and other mining companies who employ sluice box gold extraction must ensure that a slope angle of 10º is used during gold extraction for optimum gold recovery rate.

References

Agyei, G. and Gordon J. (2017), "Effect of Riffle Height and Spacing of a Sluice Board on Placer gold recovery", *Ghana Mining Journal*, Vol. 17, No. 1, pp. 64 – 72.

Alabi O.O. and Gbadamos Y.E. (2021), "Investigating the Potentials of Sluice Box Angle of Tilt on the Beneficiation of Birnin-Gwari Gold Deposit", *UOYE Journal of Engineering and Technology*, Vol. 6, No. 2, pp 88 – 91.

Banisi, S. and Hadizadeh, M. (2008), "A review on the physical separation of gold from its ores", *Minerals Engineering*, Vol. 21, No.3, pp. 238-249.

Hamilton, J.F. (1988), "A Study of the Fine Gold Recovery of Selected Sluice box Configurations", *MSc Thesis report*, University of Altberta, Canada, 97pp.

Hilson, G. (2002), "Artisanal gold mining in Ghana: An assessment of environmental and social impacts", *Natural Resources Forum*, Vol. 26, No. 4, pp. 292-300.

Kelly, P. E., Whiten, W. J., & Mular, A. L. (1995), "Optimisation of pulsating jig design and operation parameters for gold recovery", *Minerals Engineering*, Vol. 8, No. 1, pp. 63-75.

Kotze, M., Green, B., Mackenzie, J. and Virnig, M. (2005), "Resin-In-Pulp and Resin-In-Solution", *Developments in Mineral Processing*, Vol. 15, No. 1, pp. 603–635.

Lam, C.K.G. and Bremhorst, K.A. (1981), "Modified Form of Model for Predicting Wall Turbulence", *ASME Journal of Fluids Engineering*, Vol.103, pp. 456-460.

Lovedayt, B. K. (1982), "Some Considerations in the Use of Gravity Concentration for the Recovery of Gold", *Journal of The South African Institute of Mining and Metallurgy*, Vol. 82, No. 5, pp. 121–124.

Mular, A. L., Herbst, J. A. and Whiten, W. J. (2002), "The effect of sluice box design on gold recovery", *Minerals Engineering*, Vol. 15, No. 10, pp. 703-710.

Oyuntsetseg, T. and Altantuya, B. (2007), "Design modification of sluice riffles", *Scientific conference of professors, Mining School of Mongolian Science and Technology University*, Ulaanbaatar.

Simmons, A. D. and Brown, K. R. (2014), "Sluice boxes as hydraulic structures for flow regulation and control" *Journal of Hydraulic Engineering*, Vol. 140, No. 7, pp. 106 -144.

Sobachkin A. and Dumnov G. (2014), "CAD CAE Integration: Meshing & Integration of Analysis into the Design Process", *NAFEMS World Congress*, Vol.1, pp. 7-9.

Stenmark E. (2013), "Multiphase Flow Models in CFD Software", *Master's Thesis Report*, Chalmers University of Technology, 61p.

Stewart, D. F. and Ramsay, P. W. (1993), "Improving the Simple Sluice Box", *International Journal of Mineral Processing*, Vol. 39, No.1, pp. 119–136.

Veiga, M. M., Metcalf, S. M., Baker, R. F., Klein, B., Davis, G., Bamber, A., Siegel, S. and Singo, P. (2006), "Manual for Training Artisanal and Small-Scale Gold Miner/Vienna, Austria: GEF/UNDP/UNIDO", *Global Mercury Project*, Vol. 1, No. 1, 144pp.

Yin**,** E. Quaicoe, E and Asiedu,E. K. (2020a) "Design of a Combined Gravity Concentration and Leaching Plant for the Small-scale Gold Mining Industry in Ghana", *Proceedings of 6th UMaT Biennial International Mining and Mineral Conference,* Tarkwa, Ghana, pp. 480-488.

Yin, E., Muvengei, O., and Kihiu, J. M., (2020b), "Conveyor Chain Links – A Review", *Proceedings of 6th UMaT Biennial International Mining and Mineral Conference,* Tarkwa, Ghana, pp.201-207.

Yin, E, Vandijk, D and Yeboah, P, "Design and Finite Element Analysis of an Automatic Electromechanical Overload Detecting System for Trucks", *Journal of Engineering, Wiley*, Vol. 2024, pp 1-11, 2024.

Authors

Edward Yin is a lecturer in the Mechanical Engineering Department at the University of Mines and Technology (UMaT), Tarkwa, Ghana. He holds a BSc (Mechanical Engineering) from UMaT and an MSc (Mechanical Engineering) from JKUAT, Kenya. His research interests include Engineering failure analysis, design optimization, computational/experimental mechanics as well as material characterization.

Ebenezer Taylor is a graduate of the University of Mines and Technology, Tarkwa and holds a Bachelor of Science Degree in Mechanical Engineering. He is currently undertaking his national service with Engineers and Planners Company Limited at Goldfields as a mechanical technician for mining equipment. His research interests are mechatronics and maintenance.

Enoch Quaicoe received the B.Sc. degree in Mechanical Engineering from the University of Mines and Technology, Tarkwa, Ghana, in 2020. He is currently an M.Sc. research student in Mechatronics and Robotics Engineering at Egypt-Japan University of Science and Technology (E-JUST), Alexandria, Egypt. His current research interests include mechatronics, robotics, soft robots, surgical robots, model predictive control, optimization, automation, machine learning, and intelligent control.

Evans Kesse Asiedu is a graduate of University of Mines and Technology, Tarkwa and holds a Bachelor of Science Degree in Mechanical Engineering. His research interests are mechatronics and automation engineering.